OMP-based hybrid precoding and SVD-based hybrid combiner design with partial CSI for massive MU-MIMO mmWave system

Alvaro Javier Ortega
Sidia Institute of Science and Technology
Manaus, Brazil
email: alvaro.ortega@sidia.com

***Abstract*—Millimeter-wave (mmWave) communications have been regarded as a key technology for the next-generation cellular systems since the huge available bandwidth can potentially provide the rates of multiple gigabits per second. Conventional precoding and combining techniques are impractical at mmWave scenarios due to manufacturing costs and power consumption. Hybrid alternatives have been considered as a promising technology to provide a compromise between hardware complexity and system performance. In this paper, we propose a hybrid precoder/combiner design through a hierarchical strategy evolving three stages. In the first stage, we incorporate the use of a low complexity and low size discrete Fourier transform based-codebook, which greatly reduces the needs of channel side information of our proposal. The hybrid precoder includes (i) a compress sensing technique, orthogonal matching pursuit(OMP), to take advantage of the channel sparsity at the beamforming selection procedure, (ii) the classical MMSE linear filter to deal with interference system, and (iii) the eigenvectors of the residual user channel to increase their channel gain. On the other hand, the hybrid combiner uses a low complex beamforming selection algorithm and the eigenvectors of their own residual channel. Numerical results in terms of BER and sum-rate illustrate the performance improvements resulting from our proposal in relation to other hybrid precoders/combiners.**

I. Introduction

MmWave communications have emerged as one of the most promising candidates for future cellular systems due to the large and underexploited mmWave band [1]. The unlicensed 60 GHz band, for example, offers 7 GHz of spectrum spanning 57 to 64 GHz in the United States [2]. However, the higher expected path loss caused by the high frequency carrier, atmospheric gases, water vapor, and atmospheric absorption result in severe link quality degradation [3]. MmWave systems need large antenna arrays to provide array gain and achieve reasonable link margin. Interestingly, packing a large number of antenna elements in a sizable space in mmWave systems is possible due to the band's short wavelength [1].

For multiple input multiple output (MIMO) systems operating in conventional cellular frequency bands, the full-digital precoder and combiner are completely realized in the digital domain by adjusting both the magnitude and phase of the baseband signals [4]. However, these conventional full-digital schemes require a dedicated expensive and energy-intensive radio frequency (RF) chain for each antenna, where an RF chain includes a low-noise amplifier, a down-converter, a digital to analog converter (DAC), an analog to digital converter (ADC) and so on, which is impractical at mmWave scenarios due to the high cost and power consumption [5]. Therefore, mmWave systems need suitable MIMO architectures and signal processing algorithms [1].

Recent work in precoding/combining designs for mmWave systems have advocated the use of hybrid architectures [1]. This technique enables spatial multiplexing transmission by using a reduced number of RF chains. The precoder/combiner is divided into the analog and digital domains. The analog domain reduces the filters dimension of the baseband system model through low-cost phase shifters, which enables full digital techniques in the digital domain [1].

A large number of hybrid precoder designs have been proposed with different approaches. [3] is one of the most popular in the literature, the authors exploit the spatial structure of mmWave channels to formulate the precoding/combining problem as a sparse reconstruction problem and they proposed the principle of basis pursuit as tool for its solution, this idea motivated other authors to continue developing hybrid precoders based on sparse reconstruction, e.g., [6]–[8]. In [9], the authors point out that maximizing the spectral efficiency can be approximated by minimizing the Euclidean distance between hybrid precoder and the full-digital precoder. However, this approach makes the hybrid precoder design becomes a matrix factorization problem difficult to deal due to the hardware constraints of analog components.

The following list summarizes the contributions of the present work:

1) To simplify the hybrid precoder/combiner design, we adopt a hierarchical strategy to divide hybrid precoding/combining problem into analog and digital parts. In this strategy, we first design the analog precoder/combiner. Then, with the analog precoder/combiner fixed, we compute the digital precoder/combiner to improve the system performance.

978-1-7281-6535-6/20/$31.00 ©2020 IEEE

2) This paper proposes a novel hybrid precoder/combiner design made by three stages, where the analog part (first stage) is designed from a finite low-side codebook, while digital part, which is divided into the second stage and third stage, applies a low-dimensional baseband precoder/combiner to manage the inter-user/symbol interference and to increase the user channel gain.
3) Even some studies, e.g., [1], [3], employ angle of departure (AoD) / angle of arrival (AoA) vectors codebooks, they are impractical, because their estimation reliability [10]–[12]. Mesh-based codebook (i.e., the beamformings are generated by linearly spaced angle breaks) are inefficient due to their large size and poor performance. Therefore, we adopt low-complexity and low-size discrete Fourier transform (DFT) based-codebooks.
4) We formulate the selection of the RF beamforming's precoder as a sum-MSE minimization problem, and propose an OMP-based algorithm to solve it.
5) Numerical results in terms of BER and sum-rate illustrate the performance improvements resulting from our proposal in relation to other hybrid precoders from the literature.

The following notation is used throughout the paper: $\mathbb{C}$ denotes the field of complex numbers; $\mathcal{A}$ is a set; $\mathbf{A}$ is a matrix; $\mathbf{a}$ is a vector; a is a scalar; $\mathbf{A}_{a,b}$, $\mathbf{A}_{a,:}$, $\mathbf{A}_{:,b}$, denote the (a,b)-th entry, a-th row, and b-th column of the matrix $\mathbf{A}$, respectively; $\mathbf{I}_N$ is the NxN identity matrix; $\mathrm{tr}\{\mathbf{A}\}$ returns the trace of matrix $\mathbf{A}$; $\| \, . \, \|_p$ is the p-norm, for the euclidean norm case, $p=2$, the under-index is avoided; $\otimes$ is the Kronecker product; $(.)^T$ and $(.)^H$ denote the transpose and conjugate transpose, respectively; $\mathbb{E}[.]$ is the expectation operator; $\mathcal{CN}(m,\sigma^2)$ denotes a complex Gaussian random variable with mean m and variance σ^2; function $\mathbf{A} = \mathrm{columnstack}\{\mathcal{A}\}$ take the elements of $\mathcal{A}$ and stack them as columns to make a matrix $\mathbf{A}$; and $[\mathbf{U}, \mathbf{\Lambda}, \mathbf{V}^H] = \mathrm{svd}(\mathbf{A})$ performs a singular value decomposition of matrix $\mathbf{A}$, such that $\mathbf{A} = \mathbf{U}\mathbf{\Lambda}\mathbf{V}^H$.

II. System model

We consider downlink mmWave MU-MIMO systems using hybrid processing in the base station (BS) and in each mobile station (MS). To enable precoding, we assume that the BS has partial channel side information knowledge. The hybrid precoder, $\mathbf{F} \in \mathbb{C}^{N_t \times KN_s}$, in the BS can be represented by the product between the RF beamformer, $\mathbf{F}_{RF} \in \mathbb{C}^{N_t \times N_{RF_t}}$, and the baseband beamformer, $\mathbf{F}_{BB} \in \mathbb{C}^{N_{RF_t} \times KN_s}$. There are K users equipped with N_r antennas and N_{RF_r} RF chains to process N_s streams. The BS has N_t antennas and sends KN_s streams simultaneously using N_{RF_t} RF chains, where N_{RF_t} satisfies $KN_s \leq N_{RF_t} \leq N_t$. If N_{RF_t} is equal to N_t, the BS performs digital beamformer [13].

Power normalization is satisfied such that $\| \mathbf{F}_{RF}\mathbf{F}_{BB} \|_F^2 = KN_s$. Then the received signal by the user k, $\mathbf{r}_k \in \mathbb{C}^{N_r \times 1}$, is expressed as

$$\mathbf{r}_k = \mathbf{H}_k \mathbf{F}_{RF} \mathbf{F}_{BB} \mathbf{s} + \mathbf{n}_k \tag{1}$$

where $\mathbf{H}_k \in \mathbb{C}^{N_r \times N_t}$ denotes the channel matrix from the BS to the user k satisfying $\mathbb{E}[\| \mathbf{H}_k \|_F^2] = N_t N_r$; $\mathbf{n}_k \in \mathbb{C}^{Nr \times 1}$ is a complex Gaussian noise vector with zero-mean and covariance matrix $\sigma_n^2 \mathbf{I}_{N_r}$, i.e., $\mathcal{CN}(0, \sigma_n^2 \mathbf{I}_{N_r})$; $\mathbf{s} \in \mathbb{Q}^{KN_s \times 1}$ is the data stream vector expressed as the concatenation of the user's stream vectors such that $\mathbf{s} = \left[\mathbf{s}_1^T, \mathbf{s}_2^T, ..., \mathbf{s}_K^T\right]^T$ with $\mathbb{E}[\mathbf{s}\mathbf{s}^H] = \mathbf{I}_{KN_s}$ and whose entries belong to a constellation $\mathbb{Q}$. The analog part of the precoder, $\mathbf{F}_{RF}$, is implemented by phase shifters, satisfying $\| \, (\mathbf{F}_{RF})_{i,j} \, \| = \frac{1}{\sqrt{N_t}}$.

The receiver uses its N_{RF_r} RF chains and analog phase shifters to obtain the processed received signal

$$\mathbf{y}_k = \mathbf{W}_{BB_k}^H \mathbf{W}_{RF_k}^H \mathbf{H}_k \mathbf{F}_{RF} \mathbf{F}_{BB} \mathbf{s} + \mathbf{W}_{BB_k}^H \mathbf{W}_{RF_k}^H \mathbf{n}_k \tag{2}$$

where $\mathbf{W}_{RF_k} \in \mathbb{C}^{N_r \times N_{RF_r}}$ is the RF combining matrix and $\mathbf{W}_{BB_k} \in \mathbb{C}^{N_{RF_r} \times N_s}$ denotes the baseband combining matrix of the user k. Similarly to the RF precoder, $\mathbf{W}_{RF_k}$ is implemented using phase shifters and therefore $\| \, (\mathbf{W}_{RF_k})_{i,j} \, \| = \frac{1}{\sqrt{N_r}}$ [3].

In order to decrease the complexity terminals, the symbol vector estimation procedure is performed by an approximation of the minimum distance detector as follows

$$\hat{\mathbf{s}}_k = \underset{\mathbf{d} \in \mathbb{Q}^{N_s \times 1}}{\arg\min} \| \, \mathbf{y}_k - \mathbf{d} \, \|^2 \tag{3}$$

such that the processed received signal is rounded to the nearest constellation symbol. In addition, the signal-to-noise ratio (SNR) is defined as

$$\begin{aligned} \mathrm{SNR} &= \frac{\mathbb{E}[\|\mathbf{F}_{RF}\mathbf{F}_{BB}\mathbf{s}\|^2]}{\sigma_n^2} \\ &= \frac{Tr\left(\mathbf{F}_{RF}\mathbf{F}_{BB}\mathbb{E}[\mathbf{s}\mathbf{s}^H]\mathbf{F}_{BB}^H\mathbf{F}_{RF}^H\right)}{\sigma_n^2} \\ &= \frac{\| \, \mathbf{F}_{RF}\mathbf{F}_{BB} \, \|_F^2}{\sigma_n^2} = \frac{KN_s}{\sigma_n^2} = \frac{E_T}{\sigma_n^2} \end{aligned} \tag{4}$$

where $E_T = KN_s$ represents the total energy available at the BS for transmission.

III. Channel model

There are two models widely used in the mmWave literature for indoor scenarios, the Saleh-Valenzuela channel model and the extended Saleh-Valenzuela geometric model. The first one considers the resulted channel as a sum of two clustered multipath, a cluster with line-of-sight (LOS) paths and other with non-line-of-sight (NLOS) paths [14], [15]. The second one captures more accurately the mathematical structure by dropping off the cluster with NLOS due to the limited scattering at high frequency and the antenna correlation in tightly packed arrays [3], [13], [16]–[18].

Thus, we considered the mmWave channel as follows [16]

$$\mathbf{H}_k = \sqrt{\frac{N_t N_r}{N_p}} \sum_{p=1}^{N_p} \alpha_{k,p} \mathbf{d}_{N_r}(\phi_{k,p}^r, \theta_{k,p}^r) \mathbf{d}_{N_t}(\phi_{k,p}^t, \theta_{k,p}^t)^H \tag{5}$$

where N_p is the number of multi-path components in the channel; $\alpha_{k,p} \backsim \mathcal{CN}(0,1)$ is the complex gain of the p-th multi-path component in the channel for the k-th user, whereas $\phi^r_{k,p}$ ($\theta^r_{k,p}$) and $\phi^t_{k,p}$ ($\theta^t_{k,p}$) are its azimuth (elevation) angles of arrival and departure, respectively [3]. We consider the use of a uniform planar array (UPA) formed by $N_t = N_{t_h} N_{t_v}$ ($N_r = N_{r_h} N_{r_v}$) antennas, N_{t_h} (N_{r_h}) antennas in the horizontal side and N_{t_v} (N_{r_v}) antennas in the vertical side, with the antenna spacing of half-wavelength at the transmitter (receiver), whose response is given by:

$$\mathbf{d}_{N_t}(\phi,\theta) = \mathbf{d}_{N_{t_h}}(\pi cos(\phi) sin(\theta)) \otimes \mathbf{d}_{N_{t_v}}(\pi cos(\theta)) \quad (6)$$

with

$$\mathbf{d}_M(\psi) = \frac{1}{\sqrt{M}} \left[1, e^{j\psi}, ..., e^{j(M-1)\psi}\right]^T \in \mathbb{C}^{M\times 1} \quad (7)$$

IV. Hybrid combiner proposal

We address the RF beamforming selection in the combiner such that maximizes the downlink channel gain as follows:

$$\begin{aligned}(\mathbf{W}_{RF_k})^*_{:,i} &= \underset{(\mathbf{w}_{RF_k})_{:,i}\in\mathcal{W}}{\arg\max} \parallel (\mathbf{W}_{RF_k})_{:,i}\, \mathbf{H}_k \parallel \quad (8)\\ &\vdots \\ (\mathbf{W}_{RF_k})^*_{:,N_s} &= \arg\max \parallel (\mathbf{W}_{RF_k})_{:,N_s}\, \mathbf{H}_k \parallel \\ &\qquad (\mathbf{w}_{RF_k})_{:,N_s}\in\mathcal{W}\backslash\{(\mathbf{W}_{RF_k})_{:,1},...,(\mathbf{W}_{RF_k})_{:,N_s-1}\}\end{aligned}$$

We design the digital par of the combiner as a two-stages filter, $\mathbf{W}_{BB_k} = \mathbf{W}^{(a)}_{BB_k}\mathbf{W}^{(b)}_{BB_k}$. For the first stage, $\mathbf{W}^{(a)}_{BB_k}$, we make use of the expression derived in [19] and rewritten as (9), which aims to maximize the sum rate system

$$\mathbf{W}^{(a)*}_{BB_k} = \underset{\mathbf{W}_{BB_k}}{\arg\max} \det\{\tilde{\mathbf{W}}^H_k \mathbf{H}_k \mathbf{H}^H_k \tilde{\mathbf{W}}_k\} \quad (9)$$

where $\tilde{\mathbf{W}}_k = \mathbf{W}_{RF_k}\mathbf{W}^{(a)}_{BB_k}$. An approach to solve the problem in (9) is to look for the product $\tilde{\mathbf{W}}^H_k \mathbf{H}_k \mathbf{H}^H_k \tilde{\mathbf{W}}_k$ be a diagonal matrix with large entries. Therefore, applying a singular value decomposition as $[\mathbf{V}_k, \mathbf{\Lambda}_k, \mathbf{V}^H_k] = \text{svd}\left(\mathbf{W}^H_{RF_k}\mathbf{H}_k\mathbf{H}^H_k\mathbf{W}^H_{RF_k}\right)$, it is possible obtain a full diagonalization of the product $\tilde{\mathbf{W}}^H_k \mathbf{H}_k \mathbf{H}^H_k \tilde{\mathbf{W}}_k$ through $\mathbf{W}^{(a)}_{BB_k} = \mathbf{V}_k$. Note that to obtain $\mathbf{W}_{RF_k}$ and $\mathbf{W}^{(a)}_{BB_k}$ the knowledge $\mathbf{H}_k$ is not required but its projections with the different beamformings of $\mathcal{W}$. The second stage, $\mathbf{W}^{(b)}_{BB_k}$, will be described in the following section in Algorithm 1.

V. Hybrid precoder proposal

In order to decrease both inter user/symbol interference, we address our hybrid precoder design as a minimization problem as follows

$$\begin{aligned}\mathbf{F}^*_{RF}\mathbf{F}^*_{BB} = \underset{\mathbf{F}_{RF},\mathbf{F}_{BB}}{\arg\min} &\parallel \mathbf{I}_{KN_s} - \mathbf{W}^H\mathbf{H}\mathbf{F}_{RF}\mathbf{F}_{BB} \parallel^2_F \quad (10)\\ \text{s.t. } &\mathbf{F}_{RF} \in \mathcal{F}, \parallel \mathbf{F} \parallel^2_F = KN_s\end{aligned}$$

where $\mathbf{W} = \text{blkdiag}\{\mathbf{W}_1, ..., \mathbf{W}_K\}$, $\mathbf{W}_k = \mathbf{W}_{RF_k}\mathbf{W}_{BB_k}$, and $\mathbf{H} = \begin{bmatrix}\mathbf{H}^T_1 & \cdots & \mathbf{H}^T_K\end{bmatrix}^T$. Note that for an ideal solution of (10) the processed received signal would be written as

$$\mathbf{y}_k = \sqrt{\gamma}\mathbf{s}_k + \mathbf{W}_k\mathbf{n}_k \quad (11)$$

where γ represents the received signal power.

In [1], a similar MSE minimization problem was derived and solved as a convex quadratic problem. However, the authors used a closed-form for the minimum mean square error (MMSE) precoder exclusive for their particular hybrid processing. A more general expression for this filter when general hybrid processing is used has been demonstrated in [19], [20]. We adopt a similar methodology to that proposed in [1] but taking into account [19], [20]. The adopted methodology takes advantage of channel sparsity through a compressing sensing technique, OMP algorithm, which uses an MMSE filter to compute its residual matrix. Our proposed solution to solve (10) is detailed in Algorithm 1. For more details about OMP algorithm, we recommend to the readers go to [1], [3], [21].

Algorithm 1 Proposed OMP-based hybrid precoder

1: **Outputs**: $\mathbf{F}_{RF}$, $\mathbf{F}_{BB}$
2: $\tilde{\mathbf{W}} = \text{blkdiag}\{\tilde{\mathbf{W}}_1, ..., \tilde{\mathbf{W}}_K\}$
3: $\mathbf{V}_{res} = \mathbf{I}_{KN_s}$
4: $\mathbf{F}_{RF} =$ Empty
5: **for** $r = 1 : N_{RF_t}$
  $\mathbf{A} = \text{columnstack}\{\mathcal{F}\}$
  $\Phi = \mathbf{A}^H\mathbf{H}^H\tilde{\mathbf{W}}\mathbf{V}_{res}$
  $k = \arg\max_l \left(\mathbf{\Phi}\mathbf{\Phi}^{\mathbf{H}}\right)_{l,l}$
  $\mathbf{F}_{RF} = [\mathbf{F}_{RF} \mid \mathbf{A}_{:,k}]$
  $\mathcal{F} = \mathcal{F} \setminus \{\mathbf{A}_{:,k}\}$
  $\tilde{\mathbf{H}} = \tilde{\mathbf{W}}^H\mathbf{H}\mathbf{F}_{RF}$
  $\mathbf{T}_B = \left(\tilde{\mathbf{H}}^H\tilde{\mathbf{H}} + \frac{\text{tr}\{\sigma^2_n\tilde{\mathbf{W}}^H\tilde{\mathbf{W}}\}}{E_T}\mathbf{F}^H_{RF}\mathbf{F}_{RF}\right)^{-1}\tilde{\mathbf{H}}^H$
  $\mathbf{V}_{res} = \dfrac{\mathbf{I}_r - \tilde{\mathbf{H}}\mathbf{T}_B}{\parallel \mathbf{I}_r - \tilde{\mathbf{H}}\mathbf{T}_B \parallel_F}$
6: $\mathbf{T}_B = \begin{bmatrix}\mathbf{T}_{B_1} & \cdots & \mathbf{T}_{B_K}\end{bmatrix}$
7: **for** $k = 1 : K$
  $\left[\mathbf{U}_k, \mathbf{D}_k, \mathbf{V}^H_k\right] = \mathbf{svd}(\tilde{\mathbf{W}}_k\mathbf{H}_k\mathbf{T}_{B_k})$
  $\mathbf{W}^{(b)}_{BB_k} = \mathbf{U}_k$
  $\mathbf{F}_{BB_k} = \mathbf{T}_{BB_k}\mathbf{V}_k$
8: $\mathbf{F}_{BB} = \begin{bmatrix}\mathbf{F}_{BB_1} & \cdots & \mathbf{F}_{BB_K}\end{bmatrix}$
9: Compute a normalization constant such that $\parallel \mathbf{F} \parallel^2_F = KN_s$.

Note that in our proposed Algorithm 1 the selected beamforming is removed from $\mathcal{F}$ in order to avoid a multiple selection and so reduce inter user interference. This important feature was not considered in the previous works [1], [3]. Furthermore, observe that to compute our proposed hybrid

precoder/combiner only partial channel side information is required, due to just the user channel projections over the beamformins are needed.

VI. Numerical Results

In the simulations, the users channels are generated with $N_p = 10$ multi-paths components, the azimuth and elevation departure angles values are given by a random variable with uniform distribution in the interval of (0,2π) and (0,π), respectively. The UPAs have square formats for both transmitter and receivers, i.e., $N_{t_h} = N_{t_v} = \sqrt{N}_t$ and $N_{r_h} = N_{r_v} = \sqrt{N}_r$. The minimum allowed setting for the number of RF chains is used for both the BS and for each MS, so that $N_{RF_t} = KN_s$ and $N_{RF_r} = Ns$. QPSK modulation is used. The results are averaged over 10^3 channel realizations for each user with 10^2 symbol vector transmissions per channel.

The considered codebooks for the analog part of both combiner and precoder can be obtained by the Kronecker product of two uniform linear array (ULA) discrete Fourier transform (DFT) beamforming vectors adequately chosen from a horizontal and vertical codebook [22]. This ULA DFT codebook can be expressed as follows

$$\mathrm{DFT}_M^N = \frac{1}{\sqrt{N_t}} \begin{vmatrix} 1 & 1 & \cdots & 1 \\ 1 & e^{j2\pi\, 1\, \frac{1}{N}} & \cdots & e^{j2\pi\, 1\, \frac{N-1}{N}} \\ \vdots & \vdots & \ddots & \vdots \\ 1 & e^{j2\pi\, (M-1)\, \frac{1}{N}} & \cdots & e^{j2\pi\, (M-1)\, \frac{N-1}{N}} \end{vmatrix} \tag{12}$$

where N represents the size of the beam codebook, and M represents the number of antenna elements for the ULA case. Thus, for a general UPA case with $N_a = N_v N_h$ antennas elements distributed N_v in the vertical side and N_h horizontal side, its codebook $\mathcal{C}$ is generated by

$$\mathcal{C} = \{\mathbf{C}_{:,1}, \mathbf{C}_{:,2}, ..., \mathbf{C}_{:,N_a}\} \tag{13}$$

where

$$\mathbf{C} = \mathrm{DFT}_{N_h}^{N_h} \otimes \mathrm{DFT}_{N_v}^{N_v} \tag{14}$$

Figure 1 compares different hybrid precoder/combiner designs in terms of BER using the following simulation settings: the BS has $N_t = 12^2$ ($N_t = 10^2$) antennas and sends $N_s = 2$ streams to $K = 4$ ($K = 8$) users equipped with $N_r = 4$ ($N_r = 16$).

Figures 2 presents the achievable sum rate results using the settings described before using the following expression

$$\sum_{k=1}^{K} \log_2 \det \left(\mathbf{I}_{N_s} + \mathbf{W}_k^H \mathbf{H}_k \mathbf{F}_k \mathbf{F}_k^H \mathbf{H}_k^H \mathbf{W}_k \mathbf{K}_k^{-1} \right) \tag{15}$$

where $\mathbf{K}_k = \sigma_n^2 \mathbf{W}_k^H \mathbf{W}_k + \sum_{\substack{j=1 \\ j \neq k}}^{K} \mathbf{W}_k^H \mathbf{H}_k \mathbf{F}_j \mathbf{F}_j^H \mathbf{H}_k^H \mathbf{W}_k$, and $\mathbf{F}_k$ is the submatrix precoder of $\mathbf{F}$ related to the user k.

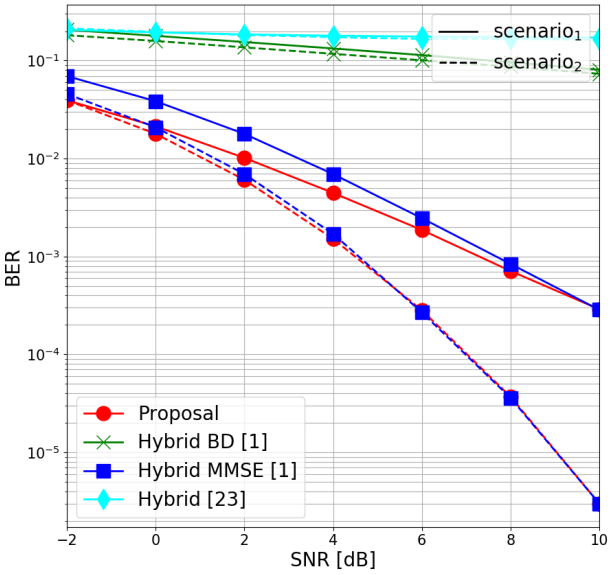

Fig. 1. BER comparison. Simulation settings: $(--)$ dashed line $N_t = 12^2$, $N_r = 4$, $N_s = 2$, $K = 4$; $(-)$ solid line $N_t = 10^2$, $N_r = 16$, $N_s = 2$, $K = 8$

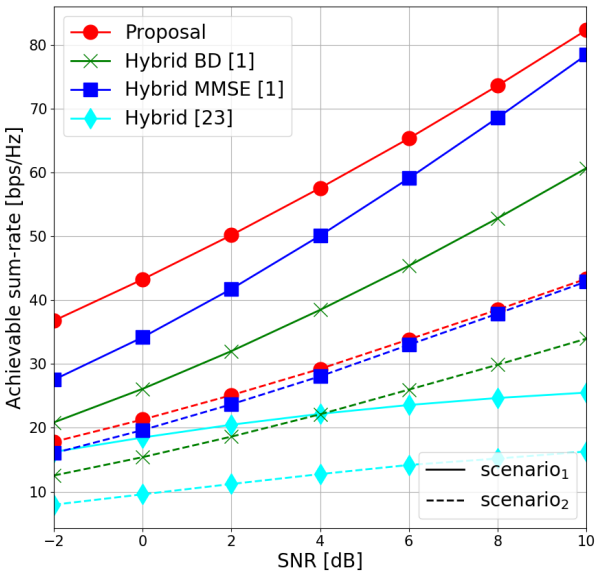

Fig. 2. Achievable sum rate comparison. Simulation settings: $(--)$ dashed line $N_t = 12^2$, $N_r = 4$, $N_s = 2$, $K = 4$; $(-)$ solid line $N_t = 10^2$, $N_r = 16$, $N_s = 2$, $K = 8$

Figures 1 and 2 evidence that our proposed hybrid precoder/combiner reaches the best BER and sum-rate, respectively, for the considered scenarios. From Figure 1 it is noted that our proposal has the better interference management

capability in the most challenging scenario (more users with low SNR value), this situation can also be evidenced in Figure 2, where our proposal greatly overcomes the other hybrid processings when the number of users is large. Furthermore, the performance of our proposal for low number of users is the best as well. Therefore, our proposal is useful for mmWave scenarios with both low and large number of users. Note that Hybrid [23] require an enormous SNR to obtain a workable BER/sum-rate, which greatly contrasts the results of our proposal. MmWave scenarios have very challenging channel conditions that produce low SNR values in the receiver, therefore, considering large SNR values to validate proposals is not useful. In addition, it is necessary to highlight that all hybrid proccessing considered in this paper use codebooks for their analog part design. This consideration improves the spectral efficiency of the system by decreasing the CSI estimation procedures [24], but in compensation it losses BER performance. Therefore, in order to have a fare comparison, hybrid processing techniques that require full CSI knowledge was not taking into account in this work. Furthermore, since mmWave systems are a promising solution to short-distance communications, simulations involving a number of users larger than 8 were not considered as well.

VII. Conclusions

We considered downlink mmWave massive MU-MIMO system using hybrid processing in both the base station and each terminal. We proposed a hybrid precoder design through a hierarchical strategy. The hybrid precoder is formulated as sparse reconstruction problem and solved by a compressing sensing technique, orthogonal matching pursuit(OMP). Our proposed OMP algorithm computes an MMSE filter to obtain the residual matrix and removes the selected beamforming from codebook in order to reduce inter-user interference. Numerical results in terms of BER and sum-rate have shown significant performance advantages of the proposed hybrid precoder/combiner in relation with other hybrid precoders/combiners considered, reaching the lower BER values in the most challenging scenarios (more users with low SNR).

Acknowledgment

This work was partially supported by Samsung Eletronica da Amazonia Ltda., under the auspice of the informatic law no 8.387/91.

References

[1] D. H. Nguyen, L. B. Le, T. Le-Ngoc, and R. W. Heath, "Hybrid MMSE precoding and combining designs for mmwave multiuser systems," *IEEE Access*, vol. 5, pp. 19 167–19 181, 2017.

[2] E. Torkildson, C. Sheldon, U. Madhow, and M. Rodwell, "Millimeter-wave spatial multiplexing in an indoor environment," in *GLOBECOM Workshops, 2009 IEEE*. IEEE, 2009, pp. 1–6.

[3] O. El Ayach, S. Rajagopal, S. Abu-Surra, Z. Pi, and R. W. Heath, "Spatially sparse precoding in millimeter wave MIMO systems," *IEEE transactions on wireless communications*, vol. 13, no. 3, pp. 1499–1513, 2014.

[4] Z. Wang, M. Li, Q. Liu, and A. L. Swindlehurst, "Hybrid precoder and combiner design with low-resolution phase shifters in mmwave mimo systems," *IEEE Journal of Selected Topics in Signal Processing*, vol. 12, no. 2, pp. 256–269, 2018.

[5] C. Hu, J. Liu, X. Liao, Y. Liu, and J. Wang, "A novel equivalent baseband channel of hybrid beamforming in massive multiuser MIMO systems," *IEEE Commun. Lett., vol. PP*, no. 99, pp. 1–1, 2017.

[6] A. Alkhateeb, O. El Ayach, G. Leus, and R. W. Heath, "Hybrid precoding for millimeter wave cellular systems with partial channel knowledge," in *Information Theory and Applications Workshop (ITA), 2013*. IEEE, 2013, pp. 1–5.

[7] J. Lee, G.-T. Gil, and Y. H. Lee, "Channel estimation via orthogonal matching pursuit for hybrid MIMO systems in millimeter wave communications," *IEEE Transactions on Communications*, vol. 64, no. 6, pp. 2370–2386, 2016.

[8] J. Mirza, B. Ali, S. S. Naqvi, and S. Saleem, "Hybrid precoding via successive refinement for millimeter wave MIMO communication systems," *IEEE Communications Letters*, vol. 21, no. 5, pp. 991–994, 2017.

[9] O. El Ayach, R. W. Heath, S. Abu-Surra, S. Rajagopal, and Z. Pi, "Low complexity precoding for large millimeter wave mimo systems," in *2012 IEEE international conference on communications (ICC)*. IEEE, 2012, pp. 3724–3729.

[10] A. Alkhateeb, O. El Ayach, G. Leus, and R. W. Heath, "Channel estimation and hybrid precoding for millimeter wave cellular systems," *IEEE Journal of Selected Topics in Signal Processing*, vol. 8, no. 5, pp. 831–846, 2014.

[11] ——, "Single-sided adaptive estimation of multi-path millimeter wave channels," in *2014 IEEE 15th International Workshop on Signal Processing Advances in Wireless Communications (SPAWC)*. IEEE, 2014, pp. 125–129.

[12] W. U. Bajwa, J. Haupt, A. M. Sayeed, and R. Nowak, "Compressed channel sensing: A new approach to estimating sparse multipath channels," *Proceedings of the IEEE*, vol. 98, no. 6, pp. 1058–1076, 2010.

[13] G. Kwon and H. Park, "A joint scheduling and millimeter wave hybrid beamforming system with partial side information," in *Communications (ICC), 2016 IEEE International Conference on*. IEEE, 2016, pp. 1–6.

[14] J. Song, J. Choi, and D. J. Love, "Common codebook millimeter wave beam design: Designing beams for both sounding and communication with uniform planar arrays," *IEEE Transactions on Communications*, vol. 65, no. 4, pp. 1859–1872, 2017.

[15] R. Guo, Y. Cai, Q. Shi, M. Zhao, and B. Champagne, "Joint design of beam selection and precoding for mmwave MU-MIMO systems with lens antenna array," in *2017 IEEE 28th Annual International Symposium on Personal, Indoor, and Mobile Radio Communications (PIMRC)*. IEEE, 2017, pp. 1–5.

[16] A. A. Saleh and R. Valenzuela, "A statistical model for indoor multipath propagation," *IEEE Journal on selected areas in communications*, vol. 5, no. 2, pp. 128–137, 1987.

[17] O. El Ayach, R. W. Heath, S. Abu-Surra, S. Rajagopal, and Z. Pi, "The capacity optimality of beam steering in large millimeter wave MIMO systems," in *2012 IEEE 13th International Workshop on Signal Processing Advances in Wireless Communications (SPAWC)*. IEEE, 2012, pp. 100–104.

[18] V. Raghavan, S. Subramanian, J. Cezanne, A. Sampath, O. H. Koymen, and J. Li, "Single-user versus multi-user precoding for millimeter wave MIMO systems," *IEEE Journal on Selected Areas in Communications*, vol. 35, no. 6, pp. 1387–1401, 2017.

[19] A. J. Ortega, R. Sampaio-Neto, and R. D. Pereira, "On hybrid precoder/combiner for downlink mmWave massive MU-MIMO systems," *Preprint Researchgate DOI: 10.13140/RG.2.2.36339.58405*, 2019.

[20] C. K. Thomas and D. Slock, "Mixed time scale weighted sum rate maximization for hybrid beamforming in multi-cell MU-MIMO systems," in *2017 IEEE Globecom Workshops (GC Wkshps)*. IEEE, 2017, pp. 1–6.

[21] J. A. Tropp and A. C. Gilbert, "Signal recovery from random measurements via orthogonal matching pursuit," *IEEE Transactions on information theory*, vol. 53, no. 12, pp. 4655–4666, 2007.

[22] Y. Xie, S. Jin, J. Wang, Y. Zhu, X. Gao, and Y. Huang, "A limited feedback scheme for 3d multiuser mimo based on kronecker product codebook," in *2013 IEEE 24th Annual International Symposium on Personal, Indoor, and Mobile Radio Communications (PIMRC)*. IEEE, 2013, pp. 1130–1135.

[23] K.-M. Chen, Y.-H. Pan, and T.-S. Lee, "Low-complexity beam selection for hybrid precoded multi-user mmwave communications," in *2018 IEEE International Conference on Signal Processing, Communications and Computing (ICSPCC)*. IEEE, 2018, pp. 1–5.

[24] A. Alkhateeb, S. Alex, P. Varkey, Y. Li, Q. Qu, and D. Tujkovic, "Deep learning coordinated beamforming for highly-mobile millimeter wave systems," *IEEE Access*, vol. 6, pp. 37 328–37 348, 2018.